Nondestructive Construction Error Detection in Large Space Structures

Norris Stubbs*
Texas A&M University, College Station, Texas
Taft H. Broome†
Howard University, Washington, D.C.
and
Roberto Osegueda‡
University of Texas at El Paso, El Paso, Texas

Continuum modeling of large space structures is extended to the problem of detecting construction errors in large space structures such as the proposed space station. First-order dynamic sensitivity equations for structures involving eigenfrequencies, modal masses, modal stiffnesses, and modal damping are presented. Matrix equations relating changes in element parameters to dynamic sensitivities are summarized. The sensitivity equations for the entire dynamical system are rearranged as a system of algebraic equations with unknowns of stiffness losses at selected locations. The feasibility of the formulation is numerically demonstrated on a simply supported Euler-Bernoulli beam with simulated construction defects. The method is next extended to large space structures modeled as equivalent continua with simulated construction defects.

Nomenclature

A = beam cross-sectional area
$\{a\}$ = nodal displacement vector
B = number of structural elements (or substructures)
$[B]$ = matrix relating nodal displacements to the average strain in an element
$[C]$ = damping matrix
$[D]$ = elasticity matrix
E = Young's modulus
$[F]$ = frequency-stiffness sensitivity matrix
$[G]$ = frequency-mass sensitivity matrix
I = second moment of area of cross section
$[K]$ = system stiffness matrix
K_r = modal stiffness for the rth mode
k_i = stiffness of ith structural element
L = length of the beam
$[M]$ = system mass matrix
M_r = modal mass for the rth mode
m_i = lumped mass at the ith node
$\{P\}$ = nodal force vector
V_c = volume of continuum
Y_r = rth modal vector
$\{Z\}$ = vector containing the fractional changes in the eigenfrequencies
$\{a\}$ = vector of fractional changes in stiffness reduction
a_i = fractional stiffness change at location i
$\{\beta\}$ = vector containing fractional change in mass
β_i = fractional change in mass at node i
$\{\epsilon\}$ = Lagrangian strain
λ_r = eigenvalue for rth mode
ξ_r = modal damping ratio for the rth mode
ω_{rd} = natural damped frequency for the rth mode
$\{\sigma\}$ = engineering stress

Received April 11, 1988; presented as Paper 88-2460 at the AIAA/ASME/ASCE/AHS 29th Structures, Structural Dynamics and Materials Conference, Williamsburg, VA, April 18-20, 1988; revision received Nov. 8, 1988.

*Associate Professor, Center for Mechanics and Materials.
†Director, Large Space Structures Institute.
‡Assistant Professor, Department of Civil Engineering.

Introduction

LARGE space structures (LSS) include, or will include, such structural types as booms, planar surfaces, antennaes, platforms, and space stations.[1,2] Because these discrete, periodic structures are characterized by many degrees of freedom, much recent research has focused on the goal of determining more efficient approaches to analyzing LSS.[3-5] In most of the literature dealing with the response of LSS, only the response of the completed structure is provided. Because of the hostility of the outer space environment, however, the possibility of a nondestructive means of automatically evaluating the integrity of LSS, as they evolve, is extremely attractive.

During the past decade, modest attention has been focused on the possibility of using changes in the vibrational characteristics of structures as an indication of structural modifications.[6-14] The vibration approach is based on the fact that, for any structure, the modal parameters (e.g., natural damped frequencies and modal damping ratios) depend only on the mechanical characteristics of the structure and not on the excitation applied to the structure.[15-18] Furthermore, the vibrational approach is attractive because vibrational characteristics can be obtained by taking measurements at only a single location on the structure. Such methods promise a means to alert operators to life-threatening structural conditions or to confirm possible structural damage. Thus, if the dynamic response of an evolving structure is monitored and if the monitored signature and the signature of the ideal structure at the same stage of construction are compared to yield structural differences between the evolving structure and the ideal structure, the structural differences can be used as a basis for assessing the location and severity of potential construction errors. However, none of the approaches proposed to date has been extended to predict efficiently the approximate location and magnitude of structural modifications in LSS modeled as equivalent continua.

This paper demonstrates how concepts from continuum modeling and structural modification can be extended to problems involving construction error detection in LSS. First, sensitivity equations resulting from a perturbation analysis of the equations of motion of a second-order dynamical system are reviewed. Second, the first-order sensitivities are expressed in terms of variations of the structural elements. Third, the sensitivity equations for all modes of the system are arranged as a system of linear algebraic equations with the locations and

magnitudes of structural error as unknowns. The formulation is tested by detecting various scenarios of construction errors simulated in a simply supported Euler-Bernoulli beam. Next, one procedure for obtaining equivalent continuum properties for repetitive structures is summarized. Finally, this procedure is used in combination with the construction error detection scheme to predict the locations and severity of simulated error in an LSS.

Theory of Construction Error Detection

Sensitivity Equations

In this study, a construction error is defined as an unintended reduction in stiffness of a structural member at one or more locations in that member. If an error-free structure has mass, stiffness, and damping matrices given by $[M]$, $[K]$, and $[C]$, respectively, and if, at a given stage of the construction, these quantities differ from the ideal values by the amounts $[\Delta M]$, $[\Delta K]$, and $[\Delta C]$, then, by perturbing the equation of motion, it can be shown that [19-22]:

$$\Delta\omega_{rd}^2/\omega_{rd}^2 = \Delta K_r/K_r - \Delta M_r/M_r - \Delta\xi_r^2/(1-\xi_r^2) \tag{1}$$

In deriving Eq. (1), proportional damping has been assumed.

If we set $z_{rd} = \Delta\omega_{rd}^2/\omega_{rd}^2, z_{r(\text{stiff})} = \Delta K_r/K_r, z_{r(\text{mass})} = \Delta M_r/M_r$, and $z_{r(\text{damp})} = \Delta\xi_r^2/(1-\xi_r^2)$, then Eq. (1) may be rewritten in the form

$$z_{rd} = z_{r(\text{stiff})} - z_{r(\text{mass})} - Z_{r(\text{damp})} \tag{2}$$

If Z_{rd} is the measured change in the natural damped frequency of a dynamical system, then $Z_{r(\text{stiff})}$, $Z_{r(\text{mass})}$, and $Z_{r(\text{damp})}$ represent the contributions resulting from changes in stiffness, mass, and damping, respectively. The quantity $Z_{r(\text{damp})}$ depends entirely on the damping ratios of the rth mode of the error-free and perturbed structures. The rth damping ratio can be estimated from frequency response functions associated with the structures by 1) identifying the frequency of maximum response of that mode (ω_r), 2) identifying the frequency change corresponding to the "half-power points" ($\Delta\omega_r$), and 3) computing the damping ratio using the formula $\xi_r = \Delta\omega_r/2\omega_r$. The quantity $Z_{r(\text{mass})}$ can be computed from any differences in mass between the two systems (which can be observed directly) and differences in the mode shapes of the two systems (which can be determined using techniques from modal analysis).[23]

Returning to Eq. (2), the sensitivities for the entire system may be expressed by the matrix equations

$$\{Z\}_d = \{Z\}_{\text{stiff}} - \{Z\}_{\text{mass}} - \{Z\}_{\text{damp}} \tag{3}$$

where, for example, $\{Z\}_d = \{Z_{1d}\ Z_{2d}\ \ldots\ Z_{Nd}\}^T$ and $\{Z\}_{\text{stiff}} = \{z_{1(\text{stiff})}\ \ldots\ Z_{i(\text{stiff})}\ \ldots\ Z_{N(\text{stiff})}\}^T$.

Dynamic Sensitivities/Element Properties Relationship

Consider an N-degree-of-freedom structure with B interconnecting structural elements (or substructures). Let the original stiffness of the ith structural element be given by k_i and the reduction in stiffness (i.e., the error) sustained by that member be given by Δk_i. Then, if we define a nondimensional measure of stiffness reduction, $a_i = \Delta k_i/k_i$, for the element and collect all such measures into a vector $\{a\} = \{a_1, \ldots, a_i, \ldots, a_B\}^T$, it can be shown (to a first-order approximation) that[22]:

$$\{Z\}_{\text{stiff}} = [F]\{a\} \tag{4}$$

where $[F]$ is an $N \times B$ sensitivity matrix that depends on the topology of the structure, the stiffness of the elements, and the error-free eigenvectors. Alternatively, the elements of the matrix $[F]$ may be thought of as follows. If unit stiffness reduction is inflected at location j of the structure, F_{ij} is equal to the fractional change $z_{i(\text{stiff})}$ of the ith eigenvalue.

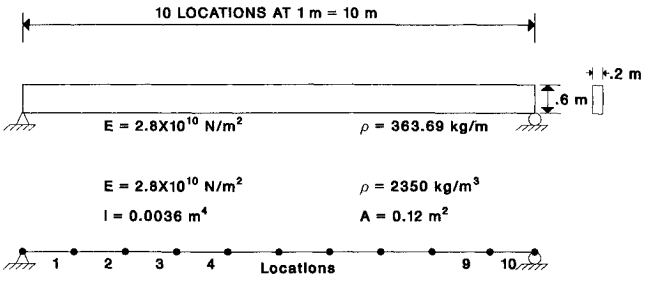

Fig. 1 Example structure and finite-element model.

Similarly, if m_i is the error-free mass at the ith node and Δm_i is the change in mass at that node, if we set $\beta_i = \Delta m_i/m_i$ and define a vector $\{\beta\}$ such that $\{\beta\} = \{\beta_1, \ldots, \beta_N\}^2$, then it can be shown that

$$\{Z\}_{\text{mass}} = [G]\{\beta\} \tag{5}$$

where the matrix $[G]$ depends on the original masses and the eigenvectors. Matrices $[F]$ and $[G]$ can be determined analytically for simple structures or via the finite-element method for more complex structures.

Problem Formulation for Construction Error Detection

This formulation is limited to problems in which the quantities $\{Z\}_d$, $\{Z\}_{\text{mass}}$, and $\{Z\}_{\text{damp}}$ can be determined experimentally and the location and severity of the construction error are sought. Accordingly, substituting Eq. (4) into Eq. (3) and rearranging, we obtain

$$[F]\{a\} = \{Z\}_d + \{Z\}_{\text{mass}} + \{Z\}_{\text{damp}} \tag{6}$$

Because the right-hand side of Eq. (6) is measurable and the matrix $[F]$ can be obtained via finite-element techniques, the vector $\{a\}$, which represents the error distribution of stiffness changes in the structure with respect to the ideal structure, can be obtained directly by solving Eq. (6). Furthermore, since the matrix $[F]$ may be nonsquare, one must resort to generalized inverse techniques to effect a solution.

Nondestructive Construction Error Detection in a Simply Supported Beam

The purpose of the exercise is to demonstrate the feasibility of the proposed technique for simple solids. The first example structure studied here is a simply supported beam and is shown in Fig. 1. In a subsequent example, the technique will be applied to LSS modeled as equivalent solids. Although only beam-type structures are used in this paper, the method can be applied to any structure that can be modeled using finite elements or matrix structural analysis. Beam-type structures are considered here not only because the mechanics of their behavior is well understood but also because beam action may be a major mode of deformation in LSS.

The elastic and geometric properties of the beam are listed in the figure along with a finite-element model of the beam used to determine numerically the dynamic bending and axial characteristics of the Euler-Bernoulli beam and the uniform rod. Given the eigenfrequencies for the error-free structure and the errant structure (i.e., the structure with the simulated error), the problem here is to predict the magnitude and location of any simulated error in the beam.

A finite-element model of the beam was subjected to a total of 14 simulated error scenarios. The first seven error cases were limited to the beam with a simulated error at only one location. The remaining scenarios, cases 8-14, considered the structure with simulated errors in two to four locations. The associated eigenfrequencies and the corresponding magnitudes

and error locations for the errant structure are summarized in Tables 1 and 2. Note that the frequencies for the errant structure were obtained by re-solving the structure with the appropriate level of error simulated. All structural analyses were performed using STRUDL.[24]

The error-sensitivity matrix $[F]$ for the structure consists of two parts: 1) an upper partitioned matrix containing the coefficients relating the 10 selected error locations to the bending frequencies, and 2) a lower partitioned matrix containing the coefficients that relate the changes in the axial frequencies to the same 10 errant locations. The coefficients for the bending portion of the matrix were determined using the mode shape vectors for a simply supported beam,

$$y_r = C \sin \lambda_r x \tag{7}$$

where C is a constant, λ_r is the rth eigenvalue given by

$$\lambda_r = r\pi/L \tag{8}$$

and L is the length of the beam. Similarly, the coefficients for the axial portion of the matrix were found by utilizing the solution for the axial modes,

$$y_r = C \sin[(r-0.5)\pi x/L] \tag{9}$$

Note that the inclusion of axial modes destroyed the symmetry about the vertical axis at the midpoint of the beam.

Note also that, in the present formulation, the fractional reduction in the bending stiffness is given by $a_{i(\text{bending})} = E(\Delta I/EI)$, where I and ΔI are, respectively, the second moment of area of the section and the simulated uniform reduction in the second moment due to the error, and E is Young's modulus. However, the corresponding fractional changes in stiffness, when the axial modes are considered, become $a_{i(\text{axial})} = E(\Delta A/EA)$, where A and ΔA are, respectively, the cross-sectional area of the section and the uniform reduction in area simulating the error. Because the two definitions of stiffness loss are related (through the radius of gyration of the section), either the axial or bending stiffness is used here, and the appropriate section of the sensitivity matrix $[F]$ is modified by a constant term that depends only on the cross-sectional properties of the beam.

In the present example, 10 possible positions of error are to be determined, and seven eigenfrequencies are used. Therefore the matrix $[F]$ has dimensions 7×10, and pseudoinverse techniques are used to obtain a solution of Eq. (6)

$$\{a_0\} = [F]^{\dagger}\{Z\}_d \tag{10}$$

in which $[F]^{\dagger}$ is the pseudoinverse of $[F]$. If no solution to $[F]\{a\} = [Z]_d$ exists, $\{a_0\}$ gives the closest possible solution. If the solution to $[F]\{a\} = \{Z\}_d$ is not unique, $\{a_0\}$ gives the solution with the minimum norm. The solution to Eq. (10) was obtained using the IMSL subroutine LLSQF.[25] Changes in mass and damping were neglected in this example.

Typical results are presented in Figs. 2–4. The results for the beam with simulated errors at a single location are displayed in Fig. 2. Typical results for the beam errant at two locations are displayed in Fig. 3. Typical results for the beam errant at three locations are shown in Fig. 4. The comparison between the predicted error and the simulated error is excellent with regard to both magnitude and location.

Table 1 Selected locations of error in a simply supported beam

Case no.	Simulated error ($\Delta I/I$) Location 1	3	5	7	10
1	0.010	0.000	0.000	0.000	0.000
2	0.000	0.010	0.000	0.000	0.000
3	0.000	0.000	0.010	0.000	0.000
4	0.000	0.000	0.000	0.010	0.000
5	0.000	0.000	0.000	0.000	0.010
6	0.000	0.000	0.100	0.000	0.000
7	0.000	0.000	0.500	0.000	0.000
8	0.010	0.020	0.000	0.000	0.000
9	0.000	0.010	0.000	0.010	0.000
10	0.010	0.000	0.010	0.010	0.000
11	0.020	0.020	0.000	0.010	0.000
12	0.010	0.020	0.000	0.020	0.010
13	0.010	0.000	0.000	0.000	0.010
14	0.020	0.000	0.020	0.010	0.010

Table 2 Eigenfrequencies for an errant beam

Error case no.	Frequencies, rad/s Bending ω_1	ω_2	ω_3	Axial ω_1	ω_2
0	58.92	234.67	524.48	543.09	1650.19
1	58.92	234.64	524.35	542.91	1649.66
2	58.89	234.44	524.22	542.94	1650.11
3	58.86	234.64	524.08	542.99	1650.03
4	58.87	234.52	524.44	543.04	1649.63
5	58.92	234.64	524.35	543.09	1650.19
6	58.29	234.37	520.24	542.01	1648.56
7	53.92	232.26	493.85	536.89	1640.82
8	58.85	234.18	523.83	542.60	1649.50
9	58.80	234.14	524.84	542.84	1648.99
10	58.81	234.46	523.92	542.76	1648.95
11	58.81	234.00	523.67	542.37	1648.42
12	58.76	233.85	523.63	542.50	1648.39
13	58.92	234.61	524.23	542.91	1649.66
14	58.75	234.38	523.38	542.47	1648.26

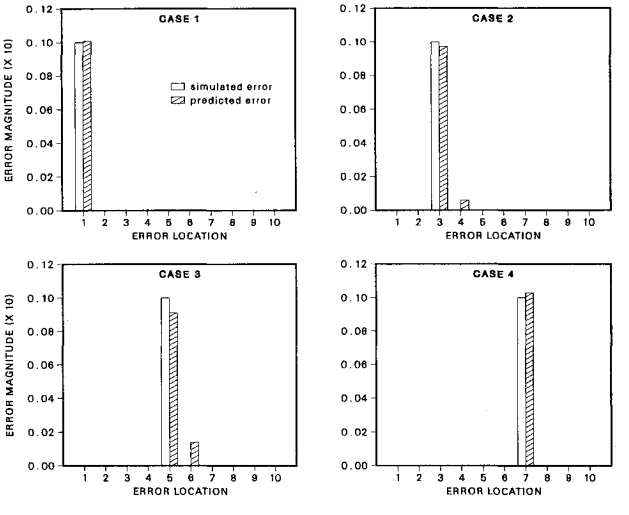

Fig. 2 Typical results for beam with error in one location.

Continuum Modeling of Large Space Structures

Many of the proposed LSS are discrete, periodic structures. Let the basic repeating unit of such a discrete structure (i.e., the unit cell), with volume and area given by V and A, respectively, be considered. The cell is composed of skeletal numbers connected at their joints. Nodal displacements and forces are denoted by vectors $\{a\}$ and $\{P\}$, respectively. These quantities are related to the system stiffness of the discrete structure, $[K_s]$, according to the equation

$$[K_s]\{a\} = \{P\} \tag{11}$$

Assuming small strains, let the elements of the continuum approximation be collected into an elasticity matrix $[D]$, such

that the engineering stress $\{\sigma\}$ is related to the Lagrangian strain $\{\epsilon\}$ by the equation $\{\sigma\} = [D]\{\epsilon\}$.

Further, let the dimensions of the continuum element be taken to be the same as those of the discrete cell. The problem then is to replace the discrete cell with some continuum characterized by $[D]$ that approximates the behavior of the discrete structural unit such that, when subjected to the same loading environment, the deformations of the two systems relate in some optimal fashion.

Many investigators[3-5,26] have developed general expressions for equivalent continuum properties of LSS subjected to arbitrary deformations. For example, energy-optimal continuum properties for a cell undergoing arbitrary deformations are given by the equation[26]

$$[D] = ([B][B]^T)^{-1}([B][K_s][B]^T)([B][B]^T)^{-1}/V_c \qquad (12)$$

Furthermore, the energy-optimal continuum properties for a discrete structure modeled as a beam may be given by[26]

$$[D_f] = ([B_f][B_f]^T)^{-1}([B_f][K_s][B_f]^T)([B_f][B_f]^T)^{-1}/(AI)_f \qquad (13)$$

the subscript f refers to the continuum properties.

Construction Error Detection in Large Space Structures Using Continuum Models

The objective here is to use the equivalent continuum properties of a discrete structure to predict the location and severity of simulated error in the discrete structure. The specific continuum property of interest here is the sensitivity matrix $[F]$ for the appropriate continuum. According to Eq. (6), for a discrete structure, the relationship between the locations and severities of error may be given by $\{Z\}_d = [F]_d\{a\}_d$ (where subscript d denotes the discrete structure). Similarly, the analogous relationship for a continuous structure may be given by $\{Z\}_c = [F]_c\{a\}_c$. If we assume isothermal conditions and that $[F]_d = [F]_c$, then the locations and severities of error in the discrete structure may be estimated using the equation

$$\{Z\}_d = [F]_c\{a\}_d \qquad (14)$$

Thus, the procedure for assessing the simulated error in a discrete structure could consist of the following steps. First, equivalent continuum properties of the discrete structure are obtained. Next, depending on the type of continuum to be modeled, e.g., a rod or a beam, the appropriate error sensitivity matrix for that continuum is developed. In the third step, the matrix containing the fractional changes in the eigenfrequencies (of the LSS) $[Z]_d$ are computed. With the matrices $[Z]_d$ and $[F]_c$ defined via measurement and analysis, $\{a\}_d$ is solved for by using Eq. (14) to determine the locations and severities of the error.

Note that Eq. (14) will yield error information only in a continuum sense. For example, if the problem is to predict the error in a large space truss modeled as a beam, this method can provide information only at the panel level; the method, as developed here, cannot predict the specific members that are errant. Despite these limitations, however, keep in mind that the method not only specifies the general location of the error but also estimates the magnitude of the discrepancy. On the basis of the information gained with this technique, detailed corrective action may now be taken.

Construction Error Detection in a Large Space Structure Modeled as an Euler-Bernoulli Cantilever

Conceivably, future LSS such as the proposed space station may be put in place by utilizing the following construction sequence. First, the major structural subsystems (which are mainly periodic discrete structures which, in turn, will support various appendages and operational modules) are assembled in space. Second, these substructures are then interconnected. Finally, appendages (e.g., solar collectors and radar dishes)

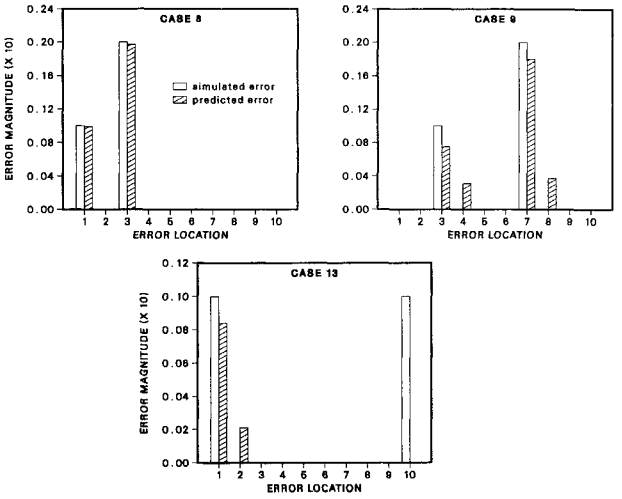

Fig. 3 Typical results for beam with error in two locations.

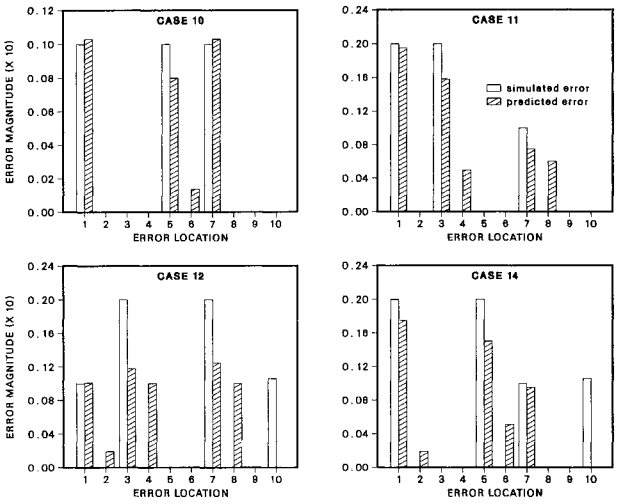

Fig. 4 Typical results for beam with error in three locations.

and special-purpose modules (e.g., specialized experimental chambers and life-supporting units) are attached to the orbiting megastructure. Note that the appendages or the modules may be attached after the first or second stage.

Because of their massive sizes, the major structural subsystems will have to be erected in space. Yet, although the building elements used to construct each structural subsystem may have exceeded quality control requirments, construction errors may occur at joints, or structural elements may be damaged during erection. The completed structural subsystem should be inspected (before final assembly of the megastructure) for conformity with expected performance. Furthermore, even if the structural subsystems are erected error-free, the completed LSS (i.e., the megastructure) should also be inspected, since the megastructure may be damaged during assembly.

The example structure, a cantilevered plane truss with 20 panels and 120 degrees of freedom, is shown in Fig. 5. The structure, for example, may represent a completed structural subsystem erected in the cargo bay of the Space Shuttle awaiting inspection before being released into orbit. All elements have identical elastic and cross-sectional properties, which are also listed in the figure. The equivalent continuum

properties for the truss (considering bending and axial behavior assuming an Euler-Bernoulli beam and a uniform rod) are also provided in Fig. 5. Given the eigenfrequencies for the error-free and the simulated errant structure (i.e., the truss), the proble is to predict the magnitude and location of numerically simulated error in the LSS.

The example structure was subjected to a total of 14 error scenarios. The scenarios were selected to demonstrate the detectability and the accuracy of the proposed approach. The first seven error cases were limited to the structure errant at only one location but with varying magnitudes of error. Cases 8–14 considered the structure errant in two to four locations.

The magnitudes and error locations for the errant structure and the associated eigenfrequencies are summarized in Tables 3 and 4. Note that the error frequencies were obtained by resolving the discrete structure with the appropriate level of error simulated. Referring to Table 3, for example, in error case 1, the bending stiffness of the first two panels was reduced by 0.01 of its original value. This change was simulated by reducing the area of the top chord by a fraction of 0.01 of its original value. The dynamic response for the truss structure is provided in the second row of Table 4. The first row in Table 4 represents the response of the error-free structure. Note also that, in this particular example, each error location in the continuum is represented by two panels in the truss. In principle, an error location in the continuum could just as easily have been represented by the region occupied by a single panel. Again, all structural analyses were performed using STRUDL.[24]

The sensitivity matrix for the cantilever was constructed similarly to the one used in the previous beam example and consists of two parts: 1) an upper partitioned matrix containing the coefficients relating the selected error locations to the bending frequencies, and 2) a lower partitioned matrix containing the coefficients that relate the changes in the axial frequencies to the errant locations. However, in this case, the coefficients for the bending portion of the matrix are computed using the mode shape vectors for a cantilever given by

$$y_r = C\{\cosh(\lambda_r x) - \cos(\lambda_r x) - k_r[\sinh(\lambda_r x) - \sin(\lambda_r x)]\} \quad (15)$$

where r is the rth mode,

$$k_r = [\cosh(\lambda_r L) + \cos(\lambda_r L)]/[\sinh(\lambda_r L) + \sin(\lambda_r L)] \quad (16)$$

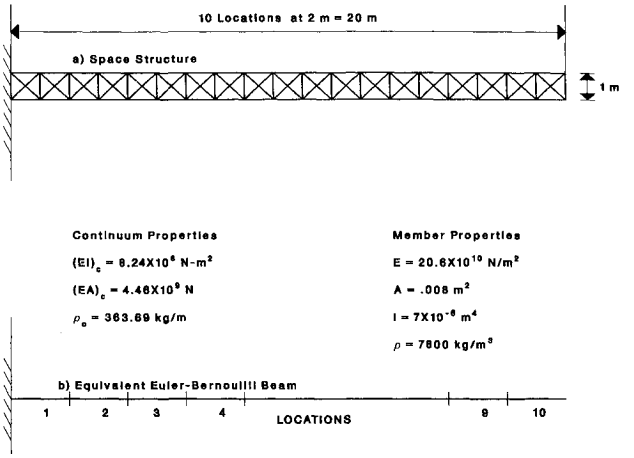

Fig. 5 Large space structure and equivalent continuum model.

Table 3 Summary of error scenarios in a large space structure

Case no.	Simulated error ($\Delta I/I$)[a] Location 1	3	5	7	10
1	0.01	0.00	0.00	0.00	0.00
2	0.00	0.01	0.00	0.00	0.00
3	0.00	0.00	0.01	0.00	0.00
4	0.00	0.00	0.00	0.09	0.00
5	0.00	0.00	0.00	0.00	0.01
6	0.00	0.00	0.10	0.00	0.00
7	0.00	0.00	0.50	0.00	0.00
8	0.01	0.02	0.00	0.00	0.00
9	0.00	0.01	0.00	0.02	0.00
10	0.01	0.00	0.01	0.01	0.00
11	0.02	0.02	0.00	0.00	0.01
12	0.01	0.02	0.00	0.02	0.01
13	0.01	0.00	0.00	0.00	0.01
14	0.02	0.02	0.00	0.01	0.00

[a] $I = h^2/2A$; h = depth of truss; A = cross-sectional area of upper or lower chord.

Table 4 Dynamic response of errant large space structure

Error case no.	Frequencies, rad/s Bending ω_1	ω_2	ω_3	ω_4	Axial ω_1	ω_2	ω_3
0	13.10	80.02	215.79	402.48	259.65	779.67	1301.88
1	13.08	79.94	215.65	402.32	259.45	779.10	1301.02
2	13.09	80.02	215.67	402.26	259.46	779.57	1301.70
3	13.09	79.96	215.77	402.23	259.52	779.50	1300.96
4	13.10	79.97	215.61	402.45	259.59	779.05	1310.71
5	13.10	80.03	215.79	402.45	259.65	779.62	1301.66
6	13.05	79.22	215.49	399.54	258.19	777.83	1291.44
7	12.70	74.36	213.63	383.96	249.68	765.79	1236.17
8	13.05	79.93	215.39	401.88	259.08	778.89	1300.66
9	13.09	79.90	215.30	402.21	259.34	778.30	1301.36
10	13.07	79.81	215.44	402.05	259.26	778.30	1299.94
11	13.03	79.78	215.05	401.69	258.82	777.71	1299.62
12	13.08	79.94	215.64	402.79	258.94	777.55	1300.10
13	13.08	79.94	205.64	402.29	259.44	779.05	1300.81
14	13.04	79.65	215.25	401.60	258.93	777.53	1297.94

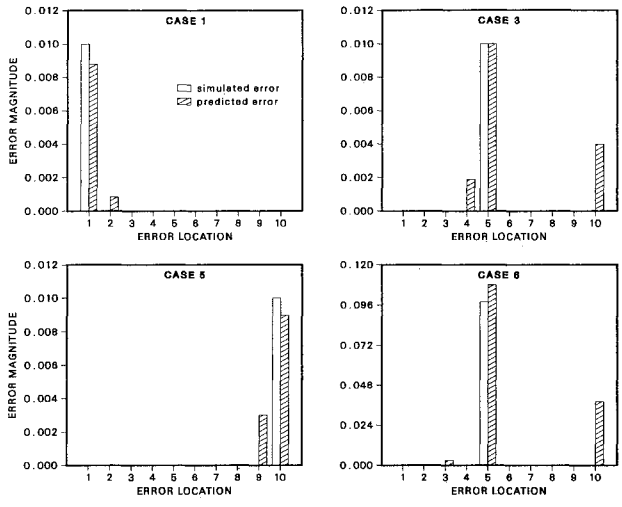

Fig. 6 Typical results for large space structure with error at one location.

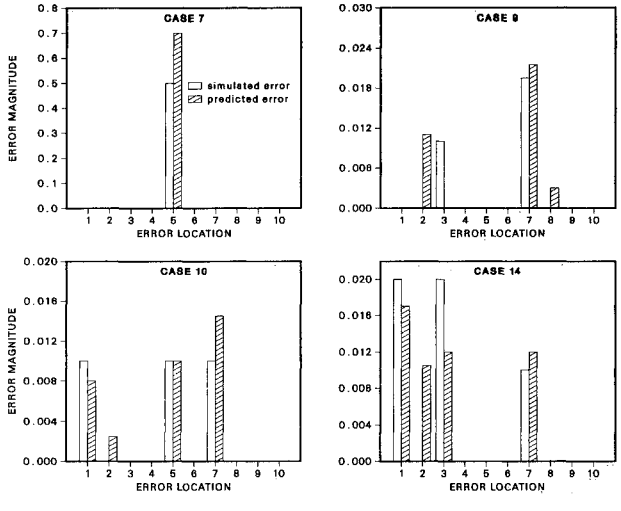

Fig. 7 Typical results for large space structure with error at multiple locations.

and the characteristic equation is given by

$$\cos(\lambda_r L)\cosh(\lambda_r L) + 1 = 0 \tag{17}$$

Once the matrix [*F*] had been determined, the solution procedure followed that of the continuum beam example studied earlier.

Typical results comparing the locations and magnitudes of the error are presented graphically in Figs. 6 and 7. For the structure with an error at a single location, in Fig. 6, it can be seen that the present formulation predicts the correct location and estimates the magnitude of the simulated error. However, false predictions may be made near a support or the free end of the structure. This is particularly true in cases 3 and 6, in which an incorrect prediction was made at location 10 (the free end).

For the structure errant at multiple locations, a similar set of observations can be made. First, the correct order of magnitude of the error is always predicted. And, in most cases, the correct location of the error is estimated. If the latter is not the case, then an adjacent location is predicted. When the structure was damaged at location 1 or 3 (see cases 9, 10, and 14), an incorrect prediction was made at loction 2.

These minor discrepancies may be resolved by using more detailed dynamic models for the LSS. Recall that the sensitivity matrix used to predict the behavior of the truss was developed using an Euler-Bernoulli beam. If an error occurred in the upper or lower chords of the structure, then the Euler-Bernoulli beam is expected to reflect the changes in the bending behavior of the truss. If an error occurred in the diagonals of a panel, a sensitivity matrix based on the Euler-Bernoulli beam most probably will not detect such a modification correctly. Such modifications can be detected, however, if sensitivity equations based on the Timoshenko beam model are used. Thus, the formulation is sensitive to modeling details, as it certainly should be. However, given the simplicity of the models used here, the results are most encouraging.

Conclusion

This paper has demonstrated how concepts from continuum modeling of LSS can be extended to problems involving construction error detection in such structures. A theory of construction error detection has been developed and applied to ordinary structural elements such as Euler-Bernoulli beams. The methodology was then extended to include construction error detection in LSS modeled as equivalent continua. A numerical example demonstrated that, with quite simple continuum models of a discrete structure, the proposed formulation predicted the correct location and magnitude of error in a beam like truss structure.

Future development of the material presented here is proceeding in several directions. Theoretically, the sensitivity matrix is being developed for the discrete structure itself and not the equivalent continuum. Each truss member will become a potential location for strucutral discrepancy. In such a formulation, prevalent fabrication errors at a given connection will show up as stiffness changes in members framing into that joint. Experimentally, data to corroborate the theory are being collected in the laboratory under controlled conditions. These experiments are designed to investigate such issues as the sensitivity of the method to the choice of mechanical model, the accuracy and detectability of the method, the constraints imposed by measurement uncertainties, and the limitations resulting from the linearization of the sensitivity equations.

Acknowledgments

This work was supported by the University Research Enhancement Program in Construction Management, Texas A&M University, and NASA Grant NAG 1-383 to the Large Space Structures Institute, Howard University. The assistance of Patricia Lombard in preparing this manuscript is greatly appreciated.

References

[1]Hagler, T., "Building Large Structures in Space," *Astronautics & Aeronautics*, Vol. 14, May 1976, pp. 56-61.

[2]Card, M. C. and Boyer, W. J., "Large Space Structures—Fantasies and Facts," *Proceedings of the AIAA/ASME/ASCE/AHS 21st Structures, Structural Dynamics and Materials Conference*, AIAA, New York, Pt. 1, 1980, pp. 101-114.

[3]Nayfeh, A. H. and Hefzy, M. S., "Continuum Modeling of the Mechanical and Thermal Behavior of Discrete Large Structures," *AIAA Journal*, Vol. 19, June 1981, pp. 766-773.

[4]Noor, A. K. and Andersen, C. M., "Analysis of Beam-Like Latice Trusses," *Computer Methods in Applied Mechanics and Engineering*, Vol. 20, Oct. 1979, pp. 53-70.

[5]Sun, C. T. and Yang, T. Y., "A Continuum Approach Toward Dynamics of Gridworks," *Journal of Applied Mechanics*, Vol. 40, March 1973, pp. 186-192.

[6]Adams, R. D., Cawley, P., Paye, C.J., and Stone, B.J., "A Vibration Technique for Non-Destructively Assessing the Integrity of Structures," *Journal of Mechanical Engineering Science*, Vol. 20, April 1978, pp. 93-100.

[7]Cawley, P. and Adams, R. D., "The Location of Defects in Structures from Measurements of Natural Frequencies," *Journal of Strain Analysis,* Vol. 14, April 1979, pp. 49–57.

[8]Chen, J. C. and Garba, J. A., "Structural Damage Assessment Using a System Identification Technique," *Structural Safety Evaluation Based on System Identification Approaches,* Vieweg, Braunschweig, FRG, 1988, pp. 474–492.

[9]Crohas, H. and Lepert, P., "Damage-Detection Monitoring Method for Offshore Platform Is Field-Tested," *Oil and Gas Journal,* Feb. 22, 1982, pp. 94, 99, 100, 103.

[10]Kenley, R. M. and Dodds, C. J., "West Sole WE Platform: Detection of Damage by Structural Response Measurements," *12th Annual Offshore Technology Conference,* Vol. 4, OTC 3866, 1980, pp. 111–118.

[11]Nataraja, R., "Structural Integrity Monitoring in Real Seas," *15th Annual Offshore Technology Conference,* Vol. 2, OTC 4538, 1983, pp. 221–228.

[12]Natke, H. G. and Yao, J. T. P., "System Identification Approaches in Structural Safety Evaluation," *Structural Safety Evaluation Based on System Identification Approaches,* Vieweg, Braunschweig, FRG, 1988, pp. 460–473.

[13]O'Brien, T. K., "Stiffness Change as a Non-Destructive Damage Measurement," *Mechanics of Nondestructive Testing,* Plenum, New York, 1980, pp. 101–121.

[14]Wojnarowski, M. E., Stiansen, S. G., and Reddy, N. E., "Structural Integrity Evaluation of a Fixed Platform Using Vibration Criteria," *9th Annual Offshore Technology Conference,* Vol. 3, OTC 2909, 1977, pp. 247–256.

[15]Gudmundson, P., "The Dynamic Behavior of Slender Structures with Cross-Sectional Cracks," *Journal of the Mechanics and Physics of Solids,* Vol. 31, Aug. 1983, pp. 329–345.

[16]Gudmundson, P., "Eigenfrequency Changes of Structures Due to Cracks, Notches or Other Geometrical Changes," *Journal of the Mechanics and Physics of Solids,* Vol. 30, Oct. 1982, pp. 339–353.

[17]Yang, J. C. S., Chen, J., and Dagalakis, N. G., "Damage Detection in Offshore Structures by the Random Decrement Technique," *Journal of Energy Resources Technology,* Vol. 106, March 1984, pp. 38–42.

[18]Yang, J. C. S., Dagalakis, N. G., and Hirt, M., "Application of the Random Decrement Technique in the Detection of an Induced Crack on an Offshore Platform Model," *Computational Methods of Offshore Structures,* American Society of Mechanical Engineers, New York, 1980, pp. 55–67.

[19]Fox, R. L. and Kapoor, M. P., "Rates of Change of Eigenvalues and Eigenvectors," *AIAA Journal,* Vol. 6, Dec. 1968, pp. 2426–2429.

[20]Wilson, R. R., "Eigenvalue-Eigenvector Solution," *Vibrations of Engineering Structures,* Springer-Verlag, New York, 1984, pp. 64–83.

[21]Stubbs, N., "A General Teory of Non-Destructive Damage Detection in Structures," *Structural Control, Proceedings of the Second International Symposium on Structural Control,* 1985, Nijhoff, Dordrecht, The Netherlands, pp. 694–713.

[22]Stubbs, N. and Osegueda, R., "Global Non-Destructive Evaluation of Offshore Platforms Using Modal Analysis," *Proceedings of the 6th International Offshore Mechanics and Arctic Engineering Symposium,* Vol. II, American Society of Mechanical Engineers, New York, 1987, pp. 517–524.

[23]Ewings, D. J., *Modal Testing: Theory and Practice,* Research Studies, Lechworth, Hertfordshire, England, 1985.

[24]*STRUDL User Manual,* McDonnell-Douglas Automation Company, St. Louis, 1984.

[25]The IMSL Library, *IMSL Inc.,* Houston, 1982.

[26]Stubbs, N. and Fluss, H., "Continuum Modelling of Discrete Structures," *Recent Advances in Engineering Mechanics and Their Impact on Civil Engineering Practice,* Vol. 1, American Society of Civil Engineers, New York, 1983, pp. 475–478.